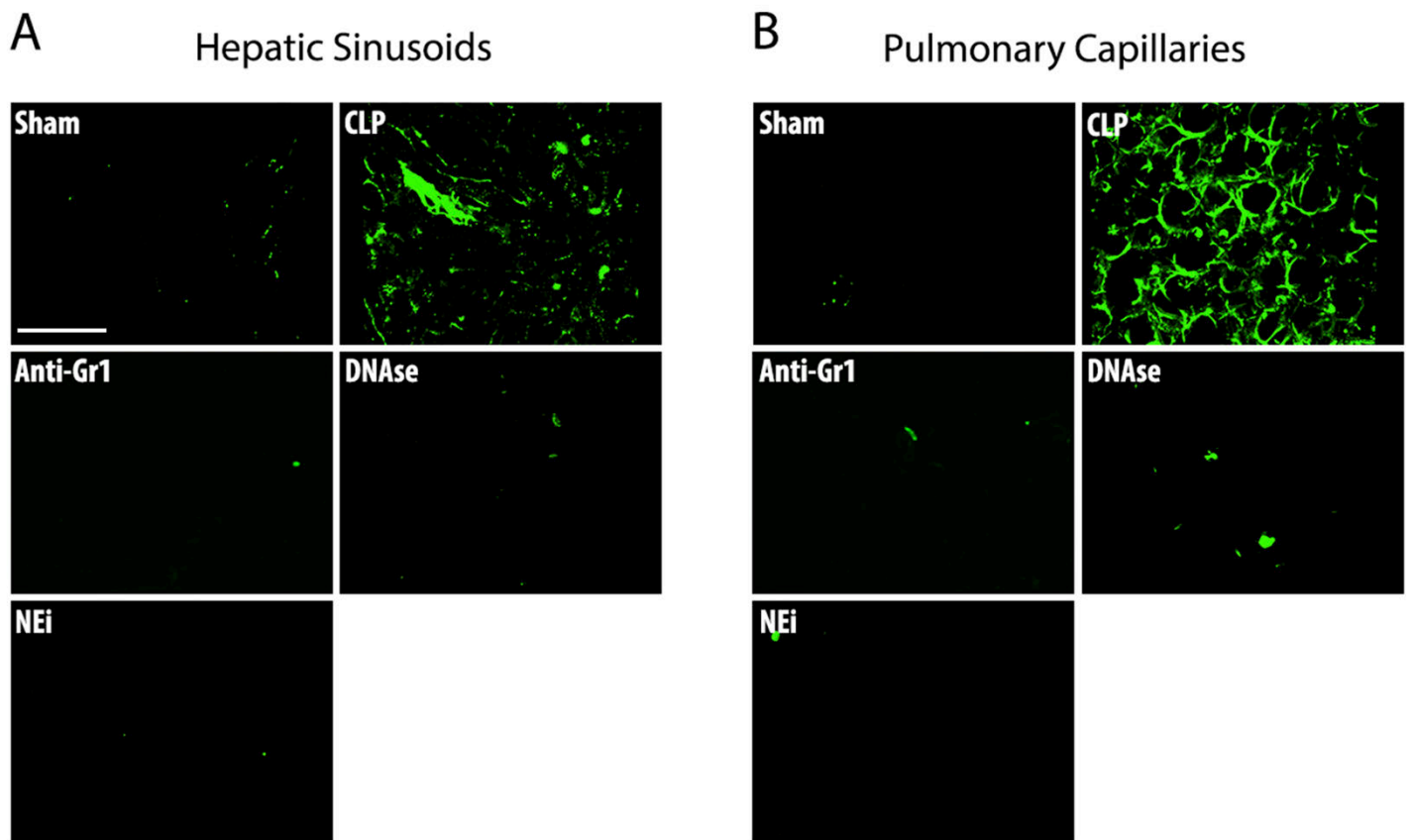


Supplemental figure 1: Extracellular DNA deposited after CLP stains positiveley for neutrophil derived granules.

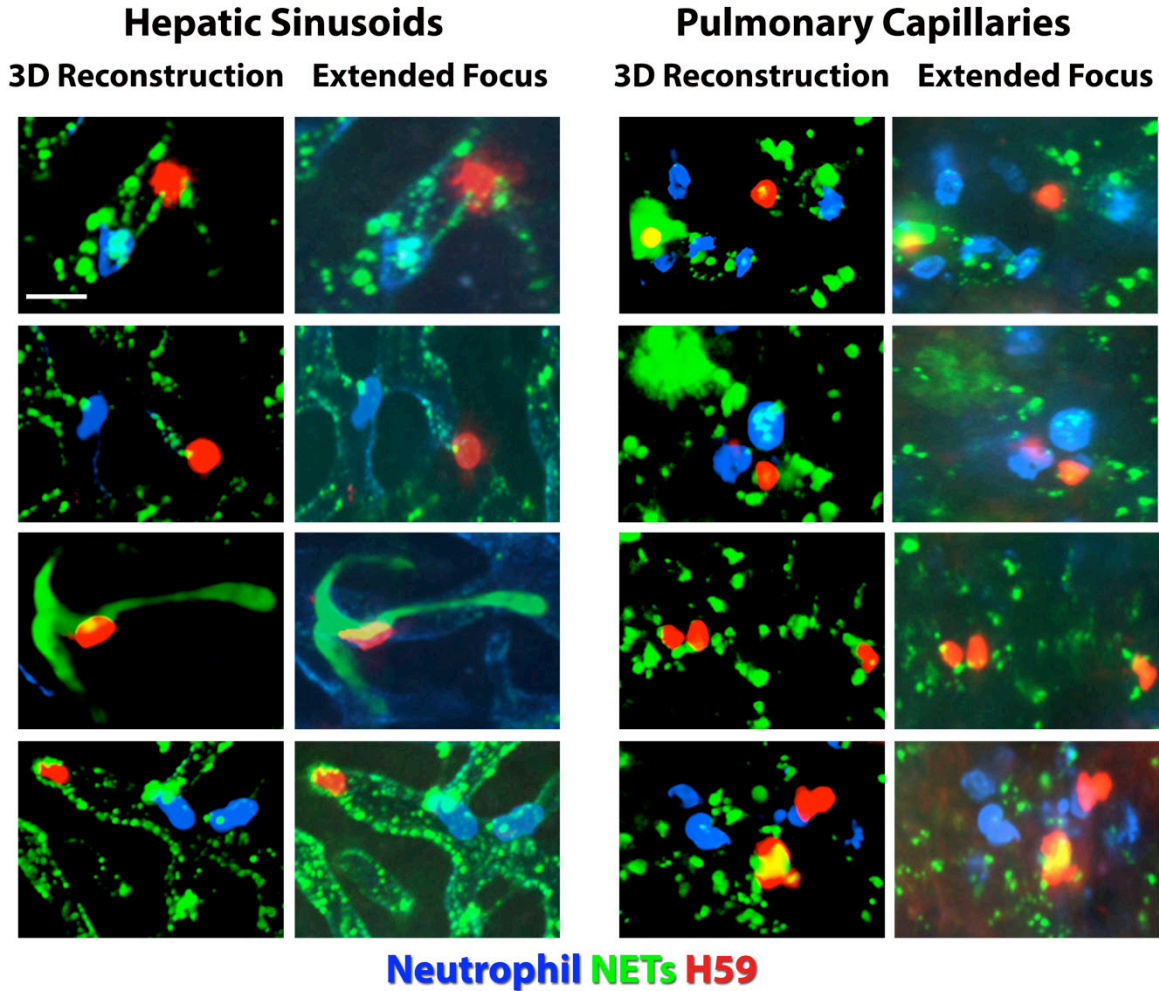
Twenty-four hours following CLP, mice were anesthetized and administered e-fluor 660 anti GR-1 (blue), Sytox green (green), and Alexa fluor 555 anti H2Ax (red) or NE (yellow) via jugular cannula. This permitted visualization of polymorphonuclear neutrophils (PMN), DNA, and H2Ax or NE respectively by employing SD-IVM in live mice after externalization of the liver. After CLP, numerous neutrophils (blue) were observed within hepatic sinusoids. Adjacent to neutrophils, DNA (green) was observed lining the hepatic sinusoidal spaces. Administration of (A) anti-H2Ax (red) or (B) anti-NE (yellow) antibodies demonstrated a staining pattern analagous to that of DNA. This suggests co-localization of these proteins within extracellular DNA, suggesting

extracellular DNA is of neutrophil origin. These findings are in accordance with what has previously been described for NETs (48). Scale bars represent 40 μ m.

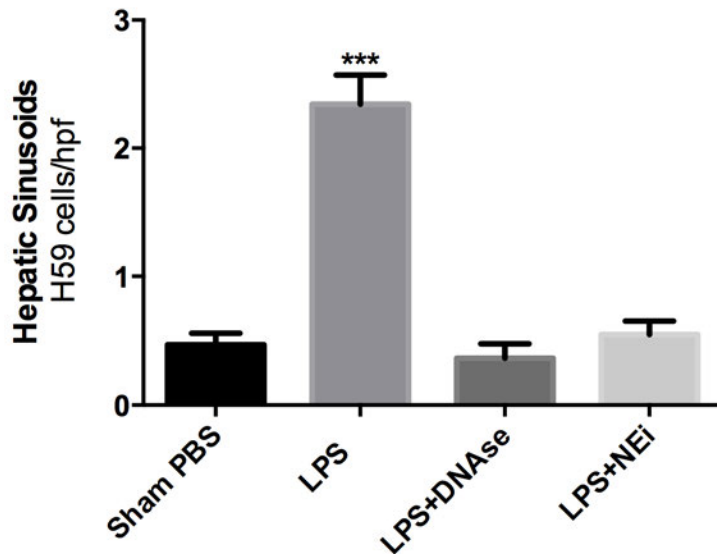


Supplemental figure 2: CLP is associated with widespread deposition of DNA within hepatic and pulmonary microvasculature.

(A, B) Representative images depicting the pattern and extent of DNA deposition within hepatic sinusoids (A) and pulmonary capillaries (B) in mice subject to sham surgery or CLP was assessed. SD-IVM was used to visualize extracellular DNA (green) after intravascular Sytox green (5 μ M) administration. DNA deposition was markedly increased in mice subject to CLP compared to sham. Neutrophil depletion with anti-GR1 antibodies (150 μ g intraperitoneal 24 hours prior to CLP), or treatment with DNase (2.5 mg/kg) or NEi (2.2 mg/kg) resulted in a visually apparent decrease in extracellular DNA deposition. Scale bars represent 85 μ m. Extracellular DNA was quantified and is presented in figure 1.

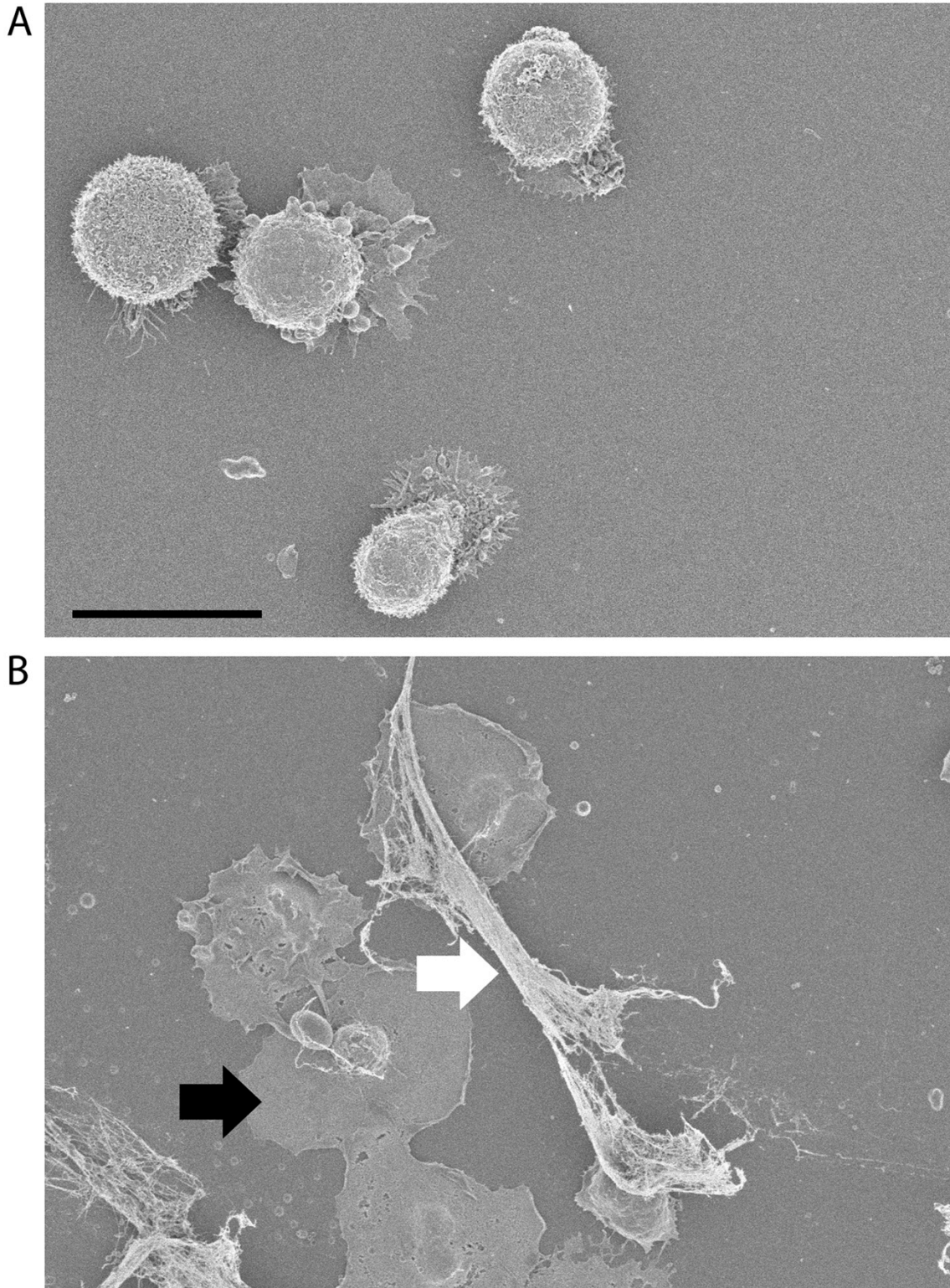


Supplemental figure 3: Circulating tumor cells arrest within neutrophil derived extracellular DNA in both hepatic and pulmonary microvasculature after CLP. Twenty four hours after CLP, mice were anesthetized and the carotid and jugular vessels were cannulated. 1×10^6 fluorescently labelled H59 cells (red) were injected via the carotid artery. Subsequently, mice received intrajugular injections of e-fluor 660 anti GR-1 (blue) and Alexa fluor 555 anti H2Ax (green) in order to visualize neutrophils (blue) and NETs (green) respectively. SD-IVM was performed permitting visualization of hepatic sinusoids in living mice or pulmonary capillaries *ex vivo* within 10 minutes. Images were captured as a series of $1 \mu\text{m}$ confocal z-stacks for a total of $\sim 10 - 20 \mu\text{m}$ (extended focus). This permitted three dimensional reconstruction so that images could be visualized in 360° (see figure 3). The extended focus and 3D reconstructions of identical images are shown side by side from liver and lung specimens for comparison. In most fields, tumor cells (red) arrested within clumps of chromatin (green) in the vicinity of neutrophils (blue). In others, tumor cells were visualized trapped within clumps of chromatin without immediately adjacent neutrophils present. This was taken to indicate DNA extrusion by trafficking neutrophils (see supplemental video 1). Scale bars represent $20 \mu\text{m}$.



Supplemental figure 4: Augmented hepatic tumor cell arrest after systemic LPS injection is abrogated by inhibitors of NET formation.

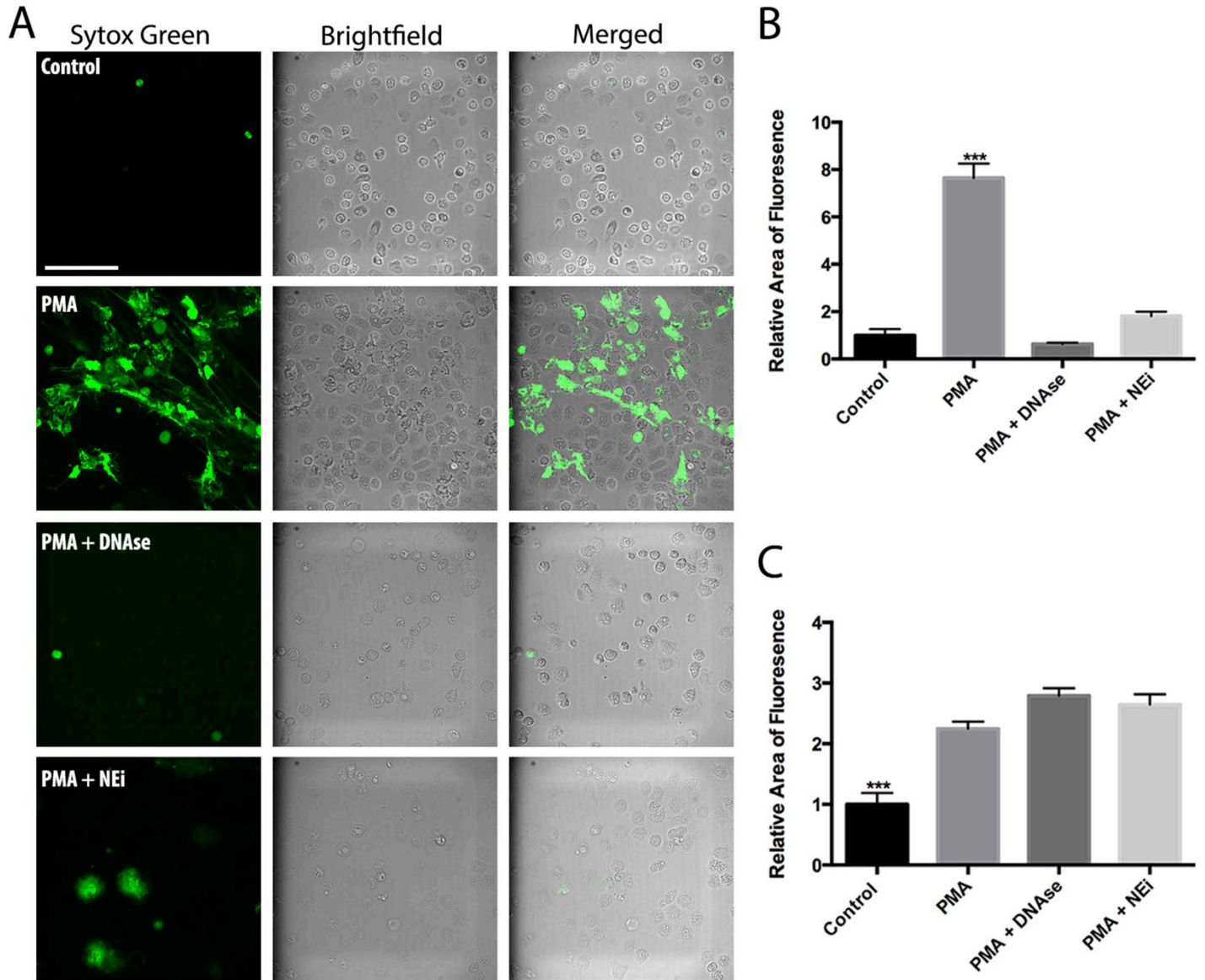
Quantification of adhesion of H59-GFP cells within hepatic sinusoids using *in vivo* epifluorescence microscopy was performed 4 hours following intraperitoneal injection of LPS or PBS (sham). 5×10^4 cells were injected via the spleen and counted in 8 high power fields 10 minutes later. Significantly more cells were adherent after LPS injection compared to PBS. In keeping with the CLP data presented in figure 3, systemic administration of DNase 1 or NEi starting 1 day prior to LPS injection abrogated adhesion to levels comparable to sham. Significance was determined using one way ANOVA with Tukey's HSD *post hoc* analysis, *** $p < 0.001$ in $n = 5$ mice per group.



Supplemental figure 5: Representative scanning electron microscopy images.

(A) A549 cells alone stimulated with 800nM PMA in absence of neutrophils in order to obtain a morphologic baseline. (B) Neutrophils 1 hour after stimulation with 800 nM

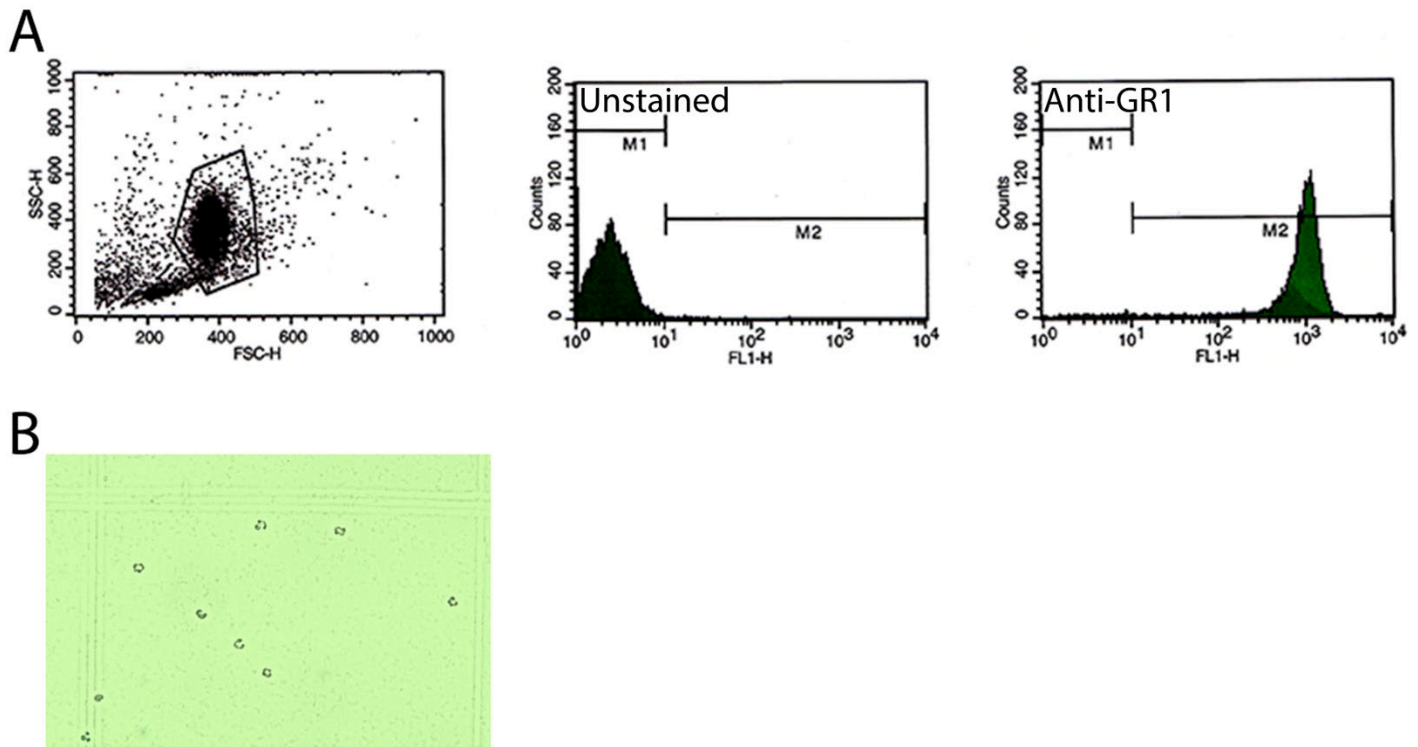
PMA in order to obtain a morphologic baseline. Note the flattening of the plasma membrane of neutrophils (black arrow) and extrusion of fibrillar NETs (white arrow). Scale bars represent 15 μm .



Supplemental figure 6: NET formation induced by PMA stimulation is abrogated by treatment of human neutrophils with DNase 1 or NEi.

(A) Representative images (20X) depicting NET formation by human neutrophils 1 hour after stimulation with 800 nM PMA alone or in the presence of 5 μ M NEi or 1000 U DNase 1. Scale bar represents 80 μ m. (B) Quantification of extracellular DNA revealed significantly increased amounts in PMA treated neutrophils compared to un-stimulated controls or neutrophils subject to DNase or NEi treatment. Decreased tumor cell adhesion *in vitro* after treatment of neutrophils with DNase 1 or NEi was attributed to ablation of NETs. In order to ensure that these differences were not the result of alterations in neutrophil adhesion, this was quantified directly (C). Prior to plating, neutrophils were fluorescently labeled (CFSE). After the termination of the static adhesion assay, the area of fluorescence in 5 high power fields (20X) was quantified. This demonstrates that PMA treatment increases neutrophil adhesion but this is

unaffected by treatment with DNase 1 or NEi. In all cases, data is represented as relative area of fluorescence compared to control and was quantified in 5 high power fields in n=3 separate experiments. Significance was determined using one way ANOVA with Tukey's HSD *post hoc* analysis,***p<0.001.



Supplemental figure 7: Bone marrow derived leukocyte isolates used for PMN re-infusion are predominantly composed of neutrophils.

(A, B) Purity of PMN yield after bone marrow isolation was achieved through flow cytometry analysis (A) and methylene blue staining (B). Flow cytometry identified a homogenous population of cells that stained positive for GR-1. Methylene blue staining demonstrated the characteristic tri-lobed nucleus present in neutrophils in >95% of isolated cells. In addition to the previous description of this method as a viable option for the isolation of murine bone marrow neutrophils, this data was taken to indicate a relatively pure neutrophil isolate.

Supplemental video 1: Tumor cell trapping occurs within areas of dense histone staining in the vicinity of neutrophils.

SD-IVM was used to acquire real time video demonstrating tumor cell arrest within suspected NETs. Mice were subject to CLP in order to induce systemic sepsis. 24 hours later, H59 cells stably expressing GFP were injected intraarterially and video acquisition was allowed to proceed over a 30-minute period. H59 cells are shown in red (GFP), neutrophils in blue (e-fluor 660 anti GR-1) and histone H2AX in green (AF-555 anti H2AX). Tumor cell arrest was noted within areas of histone staining in the vicinity of, but not in direct contact with neutrophils.